International Journal of Engineering Research & Technology (IJERT)
ISSN: 2278-0181
Vol. 14, Issue 09, RTMSE-2026

Comparative Aerodynamic Analysis of High-Lift, Efficiency-Optimized, and Conventional Airfoils for Mission-Specific Small UAV Design

Ayush Sharma[1], Himanshu Mishra[2], Harmesh Kumar[3]

[1]*B.Tech. Student, Dept. of Aerospace Engineering, Punjab State Aeronautical Engineering College, Patiala, Punjab, India*
ayush5406sharma@gmail.com

[2,3]*Assistant Professor, Dept. of Aerospace Engineering, Punjab State Aeronautical Engineering College (MRSPTU Bathinda), Patiala, Punjab, India*
himanshm08@gmail.com;harmesh.kr1@gmail.com

***Abstract* — Small unmanned aerial vehicles (UAVs) operating at low Reynolds require careful airfoil selection to meet mission-specific objectives, yet direct comparative data under unified test conditions remain scarce. This study presents a systematic numerical comparison of three representative airfoils, namely the Selig S1223 (high-lift), Eppler E205 (efficiency-optimized), and NACA 4412 (conventional baseline), at Reynolds Number of 300,000 using XFLR5. By maintaining identical solver settings across all profiles, the study isolates geometric effects and enables direct performance ranking. Simulations across angles of attack from −4° to 15° reveal distinct performance characteristics: the S1223 achieves the highest lift coefficient of 1.50 at an angle of attack 2.8°, while the NACA 4412 achieves the highest aerodynamic efficiency, with a maximum value of 90.93 at an angle of attack of 5.0°. This is 55% higher than the Eppler E205's peak of 58.62. The results establish a practical selection framework: S1223 for payload-intensive and short take-off operations, NACA 4412 for maximum endurance and range, and the Eppler E205 provides stable and predictable performance.**

Keywords: Low Reynolds number; XFLR5; UAV aerodynamics; Airfoil selection; Selig S1223; Eppler E205; NACA 4412

I. Introduction

The proliferation of small unmanned aerial vehicles for surveillance, precision agriculture, and environmental monitoring has intensified demand for aerodynamic configurations tailored to low-Reynolds-number flight regimes [1]. Unlike conventional aircraft, small UAVs typically operate at Reynolds numbers between 10^4 and 10^6, where viscous effects dominate and flow phenomena such as laminar separation bubbles and premature boundary-layer transition can severely degrade lift characteristics and amplify drag [2].

Recognizing these challenges, researchers have developed specialized airfoil geometries. Selig and colleagues pioneered high-lift profiles such as the S1223, employing aggressive aft-loading to sustain flow attachment at high angles of attack [3]. Kumar et al. [4] subsequently validated the S1223's suitability for vertical take-off and landing (VTOL) platforms requiring substantial lift during transition phases. In parallel, Mishra and Verma [5] investigated aeroelastic interactions at Re = 3×10^5, mapping how aerodynamic loading induces structural deformation. Meanwhile, efficiency-oriented profiles like the Eppler E205 have gained attention for endurance applications, where minimizing drag over extended cruise segments is paramount. Zhang et al. [6] proposed a rapid airfoil selection framework categorizing profiles as high-lift, efficiency-oriented, or baseline; yet the framework's application requires comparable performance data that is often absent from the literature.

Herein lies the motivation for the present work. While individual airfoil studies abound, they are conducted under disparate numerical settings, Reynolds numbers, and software environments, making cross-profile comparisons unreliable. A UAV designer seeking to choose between a high-lift geometry and an efficiency-optimized alternative cannot directly compare published results because differences in solver configuration may obscure true geometric performance differences. The present study addresses this gap by evaluating three representative airfoils (Selig S1223, Eppler E205, and NACA 4412) within a unified XFLR5 framework at Re = 3×10^5. By holding all numerical parameters constant, the study isolates the effect of airfoil geometry on performance, yielding reliable *relative rankings* suitable for design selection. The specific objectives are: (1) to quantify lift, drag, and aerodynamic efficiency across a range of attacks under identical conditions; (2) to identify the angle-of-attack regimes where each airfoil excels relative to the others; and (3) to establish mission-specific selection guidance for small UAV applications.

II. METHODOLOGY

2.1 Airfoil Selection and Geometry

Three airfoils were selected to represent distinct low-Reynolds-number design philosophies. The **NACA 4412** serves as a baseline, with 4% camber at 40% chord and 12% maximum thickness, representing a conventional profile without specific low-Re optimization. The **Eppler E205** features a streamlined geometry with reduced thickness and a flatter lower surface designed to minimize viscous losses over extended cruise. The **Selig S1223** represents the high-lift category, characterized by aggressive camber, a deeply concave lower surface, and a

International Journal of Engineering Research & Technology (IJERT)
ISSN: 2278-0181
Vol. 14, Issue 09, RTMSE-2026

reflexed trailing edge. This geometry is explicitly engineered to maximize lift coefficient at low speeds.
Coordinate files for each airfoil were obtained from the UIUC Airfoil Database and inspected for continuity before import into XFLR5. Figure 1 illustrates the geometric profiles, highlighting the progression from the moderate camber of the NACA 4412 to the extreme curvature of the S1223.

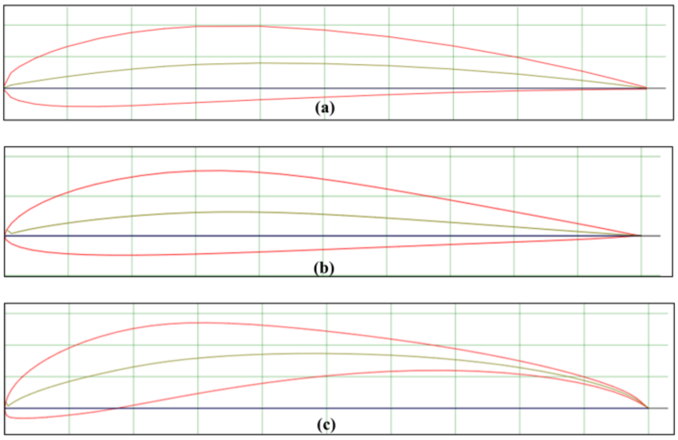

Figure 1. Geometric profiles: (a) NACA 4412, (b) Eppler E205, (c) Selig S1223.

2.2 Numerical Setup

All simulations were performed using XFLR5 (v6.57), which couples the XFOIL viscous panel method with boundary-layer analysis. This combination is well-suited to predict lift, drag, and transition behavior at low Reynolds numbers. A fixed Reynolds number of 3×10^5 was adopted to represent typical small UAV cruise conditions at flight speeds of 10–20 m/s. The angle of attack was swept from −4° to 15° capturing both attached-flow performance and pre-stall behavior. Default transition settings ($N_{crit} = 9$) were employed, corresponding to low-turbulence wind-tunnel or calm atmospheric conditions. All other parameters, including fluid properties, and panel resolution, were held constantly across all three airfoils to ensure direct comparability.

It should be noted that the primary objective of this study is *relative* performance comparison rather than absolute prediction. While panel-method solvers may exhibit deviations from experimental values depending on turbulence modeling and transition criteria, the use of identical settings across all airfoils ensures that the *comparative rankings and performance trends* remain valid for design selection purposes.
.

III. RESULTS AND DISCUSSION

3.1 Lift Characteristics

Figure 2 presents the lift coefficient (C_L) as a function of angle of attack. The Selig S1223 dominates the high-lift regime, achieving $C_{L,\,max} = 1.50$ at α = 2.8°, nearly double the NACA 4412's lift ($C_L \approx 0.75$) at the same angle. Notably, the S1223 generates substantial positive lift even at negative incidence, reflecting its aggressive camber line. This characteristic is advantageous for payload-intensive missions where high lift must be sustained during low-speed manoeuvring or short take-off runs. In contrast, the Eppler E205 exhibits a more gradual lift curve, reaching $C_L = 1.0$ only at α = 7.2°. This delayed lift buildup reflects robust flow attachment and predictable stall margins, which are desirable traits for autonomous platforms requiring stable control authority across varying flight conditions. The NACA 4412 occupies the middle ground, achieving $C_L = 1.0$ at α = 5.0°, with a linear lift slope typical of conventional airfoils.

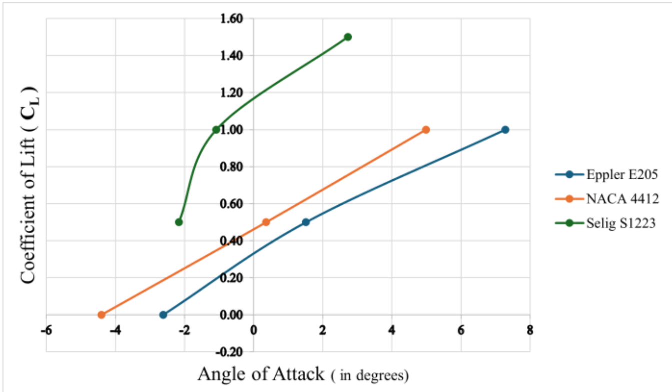

Figure 2. Lift coefficient (C_L) versus angle of attack (α) for the three airfoils at Re = 3×10^5.

3.2 Drag Characteristics

The drag coefficient (C_D) trends in Figure 3 reveal the trade-off inherent to high-lift geometries. The Selig S1223 incurs the highest drag penalty, peaking at $C_D \approx 0.041$ at α = −2.2°, a consequence of its pronounced camber strengthening adverse pressure gradients along the suction surface. At cruise-relevant angles (α = 3°–6°), the S1223's drag remains approximately 2–3 times that of the other profiles.

The Eppler E205 maintains the lowest drag across the tested range, achieving $C_{D,min} = 0.009$ at α = 1.5°. Its streamlined geometry and optimized pressure recovery delay flow separation, making it well-suited for endurance applications where minimizing energy expenditure is critical. The NACA 4412 achieves a comparable minimum drag ($C_{D,min} = 0.0084$ at α = 0.4°) but exhibits a steeper drag rise at higher angles, reflecting its lack of low-Re optimization.

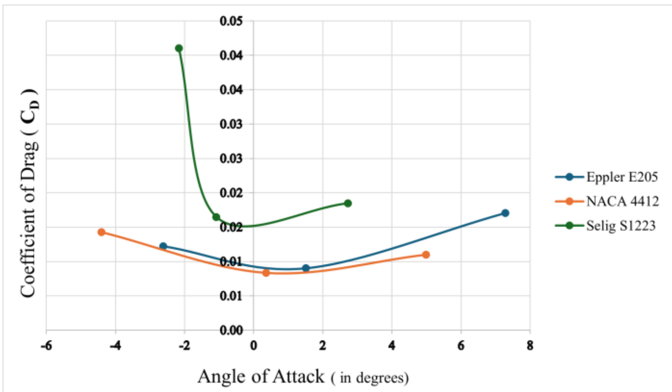

Figure 3. Drag coefficient (C_D) versus angle of attack (α) for the three airfoils.

International Journal of Engineering Research & Technology (IJERT)
ISSN: 2278-0181
Vol. 14, Issue 09, RTMSE-2026

3.3 *Aerodynamic Efficiency*

Figure 4 illustrates the aerodynamic efficiency (C_L/C_D), which combines lift and drag into a single value that influences range and endurance. The NACA 4412 has the highest peak efficiency of 90.93 at $\alpha = 5.0°$. This is 12% better than the Selig S1223 (81.27 at $\alpha = 2.8°$) and 55% better than the Eppler E205 (58.62 at $\alpha = 7.2°$). Because of this significant efficiency advantage, the NACA 4412 is the best choice for missions that need long range and endurance.

The S1223 is less efficient than the NACA 4412, but it is still efficient and reaches its highest point at a very low angle of attack. This feature is useful for missions that need a lot of lift at almost level flight attitudes, like spraying crops or deploying a payload, where keeping the fuselage pitch low is important. The Eppler E205, on the other hand, has the lowest peak efficiency of the three airfoils. However, it has smoother aerodynamic properties and a gradual lift development, making it better for situations where stable and predictable performance is more important than maximum efficiency.

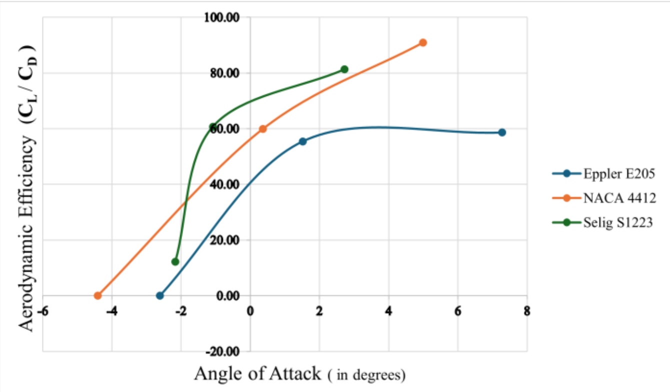

.
Figure 4. Aerodynamic efficiency (C_L/C_D) versus angle of attack (α).

3.4 *Comparative Summary*

Table 1 consolidates the key performance metrics, enabling direct comparison for design purposes. The data underscore the fundamental trade-off: the S1223 maximizes lift at the expense of drag, the NACA 4412 maximizes efficiency at the expense of peak lift, and the Eppler E205 provides smooth aerodynamic characteristics and stable performance but does not achieve the highest efficiency. Critically, these *relative rankings*, derived under identical numerical conditions, provide actionable guidance regardless of any systematic offset between predicted and experimental absolute values.

Table 1. Comparative aerodynamic performance at $Re = 3 \times 10^5$.

Airfoil	$C_{L,max}$	$C_{D,min}$	$(C_L/C_D)_{max}$	Recommended Application
Selig S1223	1.50 (α = 2.8°)	0.041	81.27	High-lift, STOL, VTOL
Eppler E205	1.00 (α = 7.2°)	0.009	58.62	General Purpose, Training
NACA 4412	1.00 (α = 5.0°)	0.0084	90.23	Endurance, cruise

IV. CONCLUSION

This study systematically compared the aerodynamic performance of the Selig S1223, Eppler E205, and NACA 4412 airfoils at $Re = 3 \times 10^5$ using a unified XFLR5-based framework. The principal findings are:

(1) The Selig S1223 delivers exceptional lift ($C_{L\ max} = 1.50$ at $\alpha = 2.8°$), making it the preferred choice for payload-critical missions, short take-off requirements, and VTOL transition phases.

(2) The Eppler E205 has a lower aerodynamic efficiency ($C_L/C_{D\_max} \approx 58.62$ at $\alpha \approx 7.2°$), but it has smoother aerodynamic behaviour and a gradual lift development, which makes it suitable for situations where stable and predictable performance is needed.

(3) The NACA 4412 has the best aerodynamic efficiency ($C_L/C_{D\ max} \approx 90.93$ at $\alpha \approx 5.0°$), making it the best choice for UAV applications that need long-lasting performance. It also offers stable and predictable aerodynamic performance.

(4) The unified comparison framework established here, with identical solver settings isolating geometric effects, provides designers with directly comparable relative performance metrics for informed airfoil selection in small UAV applications.

Future work should extend this analysis through wind-tunnel validation to correlate relative rankings with absolute experimental values, investigate surface roughness and turbulator effects, and incorporate higher-fidelity CFD methods with transition modeling to refine predictions near stall.

V. ACKNOWLEDGEMENT

The authors acknowledge the guidance and support provided by the faculty of the Department of Aerospace Engineering, Punjab State Aeronautical Engineering College, Patiala, during this study. The authors also appreciate the academic environment and institutional facilities that enabled the completion of this research work.

VI. REFERENCES

[1] Y. Lian, W. Shyy, D. Viieru, Membrane wing aerodynamics for micro air vehicles, Prog. Aerosp. Sci. 39 (2003) 425–465.

[2] J. AlMutairi, A. AlQadi, R. Prosser, Dynamics of laminar separation bubble over a NACA 0012 airfoil, Aerosp. Sci. Technol. 68 (2017) 193–204.

[3] J. Winslow, J.J. McGranahan, M.S. Selig, J.L. McMasters, Basic understanding of airfoil characteristics at low Reynolds numbers, Proc. AIAA Aerosp. Sci. Meeting, AIAA, 2018.

[4] A. Kumar, S. Verma, R. Singh, Structural and aerodynamic investigation of S1223 airfoil for high-load VTOL UAV applications, Aerosp. Syst. (in press)

International Journal of Engineering Research & Technology (IJERT)
ISSN: 2278-0181
Vol. 14, Issue 09, RTMSE-2026

[5] R.K. Mishra, A. Verma, Aerodynamic and bending analysis of low-speed airfoils at Reynolds number 300,000, Int. J. Aerosp. Eng. (2023) 1–14.

[6] J. Zhang, Y. Li, H. Chen, Fast airfoil selection methodology for small unmanned aerial vehicles at low Reynolds numbers, Appl. Sci. 12 (2022) 1–19.